

Incorporating remotely-sensed snow albedo into a spatially-distributed snowmelt model

Noah P. Molotch

Department of Hydrology and Water Resources, University of Arizona, Tucson, Arizona, USA

Thomas H. Painter

National Snow and Ice Data Center, University of Colorado, Boulder, Colorado, USA

Roger C. Bales

Division of Engineering, University of California, Merced, California, USA

Jeff Dozier

Donald Bren School of Environmental Science and Management, University of California, Santa Barbara, California, USA

Received 12 November 2003; revised 22 December 2003; accepted 31 December 2003; published 13 February 2004.

[1] Basin-average albedo estimated from remotely-sensed Airborne Visible/Infrared Imaging Spectroradiometer (AVIRIS) data specific to the catchment typically differed by 20% from albedo estimated using a common snow-age-based empirical relation. In some parts of the basin, differences were as large as 0.31. Using the AVIRIS albedo estimates in a distributed snowmelt model that explicitly includes net solar radiation resulted in a much more accurate estimate of the timing and magnitude of snowmelt as compared to the same model with the empirical albedo (R^2 of 0.73 versus 0.59 and magnitude error of 2% versus 36%). Model improvement was most significant in areas and at times where incident solar radiation was relatively high and temperatures low. *INDEX TERMS:* 1863 Hydrology: Snow and ice (1827); 1860 Hydrology: Runoff and streamflow; 1878 Hydrology: Water/energy interactions. *Citation:* Molotch, N. P., T. H. Painter, R. C. Bales, and J. Dozier (2004), Incorporating remotely-sensed snow albedo into a spatially-distributed snowmelt model, *Geophys. Res. Lett.*, 31, L03501, doi:10.1029/2003GL019063.

1. Introduction

[2] In modeling the spatial distribution of snowmelt in alpine terrain, uncertainty in snow-surface albedo can be more important than uncertainty in either air temperature [Blöschl, 1991] or snow water equivalent (SWE) [Blöschl et al., 1991]. The parameterization of snow-surface albedo in land-surface schemes has a dramatic influence on the accuracy of model-calculated snowpack energy absorption. Spectrally-integrated albedo can be estimated with data from the Airborne Visible/Infrared Imaging Spectrometer (AVIRIS) with an RMSE of 1.8% [Painter et al., 2003]. To date remotely-sensed albedo has not been incorporated into snowmelt modeling because estimation of albedo with operational sensors is problematic. Algorithms using Moderate-Resolution Imaging Spectroradiometer (MODIS) data are currently being refined for snow albedo [Klein and Stroeve, 2002]. Thus, assessing the potential utility of

these data to snow/atmosphere energy exchange models is paramount.

[3] In this study we use remotely-sensed albedo estimates from AVIRIS to assess the potential improvement in modeling the timing, magnitude and spatial distribution of snowmelt in an alpine catchment. Three questions were addressed: i) how well does a commonly used empirical albedo estimation method compare with the estimates based on AVIRIS albedo observations over the snowmelt season, ii) does using the AVIRIS-derived albedo improve estimates of snowmelt across a catchment, and iii) under what physiographic conditions across the catchment is the improvement greatest?

2. Methods

[4] The study was carried out in the 19.1 km² Tokopah basin, Sierra Nevada, California (36°36'N, 118°40'W). Elevations range from 2629 to 3487 m (Figure 1).

[5] We mapped snow albedo from 3 AVIRIS scenes (05 May, 21 May, and 18 June 1997) at a 17-m resolution using a multiple-endmember snow-covered-area and grain-size model [Painter et al., 2003]. Albedo measurements were resampled to 30-m resolution to match the resolution of the digital elevation model. During time periods without snowfall between two AVIRIS acquisitions daily pixel-specific albedo estimates were obtained by linearly interpolating albedo as a function of time. For time periods when snowfall occurred between two acquisitions, daily albedo was estimated using a linear AVIRIS albedo decay function (AADF) that we derived using the AVIRIS-observed pixel-specific albedo and the snow age at the time of observation. Snow age was determined from precipitation and temperature data from the meteorological stations in the catchment (Figure 1). Pixel-specific albedo estimates were obtained from the AADF as follows:

$$y_h = y_i - [(y_i - y_j)/(x_i - x_j)] \times [x_i - x_h] \quad (1)$$

Where y_h is the estimated albedo for snow age x_h , y_i and y_j are AVIRIS-observed albedo values for acquisitions corresponding to snow ages x_i and x_j respectively. After a

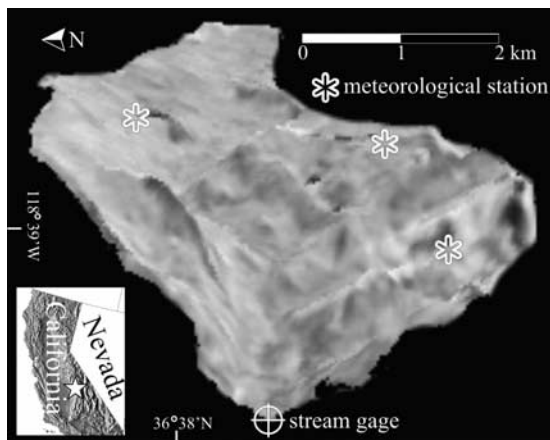


Figure 1. Landsat Thematic Mapper band 4 composite of the Tokopah basin draped over a 30-m digital elevation model. Three-dimensional perspective is looking up-valley to the east.

snowfall event the AADF was reset to the maximum AVIRIS-observed albedo value; snow albedo tends to be fairly uniform immediately after snowfall - becoming spatially heterogeneous as metamorphic processes occur at spatially-variable rates. For comparison, basin-average albedo was estimated as a function of snow age using a

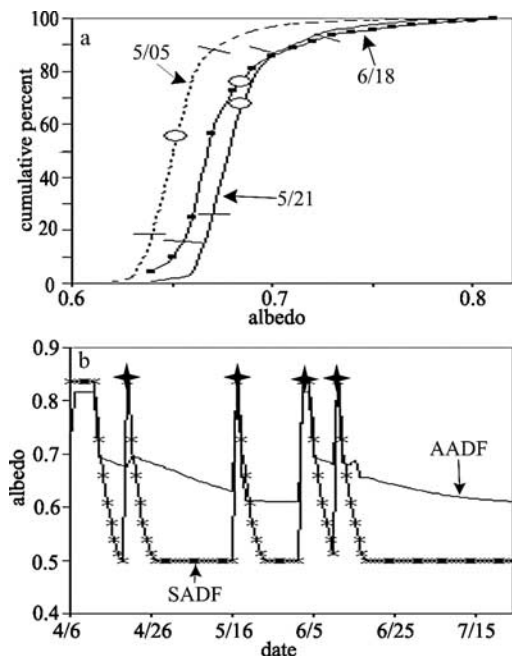


Figure 2. (a) Cumulative percent of watershed area with stated albedo for the 3 AVIRIS acquisitions. Circles indicate mean basin albedo, and perpendicular hash-marks indicate standard deviations. (b) The variation of mean basin albedo with time using the standard albedo decay function (SADF) [U.S. Army Corps of Engineers, 1956] and the AVIRIS-albedo decay function (AADF). The SADF was reset to its initial value at each snowfall event. The AADF was reset as well unless an AVIRIS acquisition occurred immediately following the snowfall event. Stars indicate snowfall events.

standard albedo decay function (SADF) [U.S. Army Corps of Engineers, 1956].

[6] Daily snowmelt was calculated from 06 April to 27 July 1997 for each 30-m grid cell using a net radiation and temperature index snowmelt model [Brubaker *et al.*, 1996]. Input data (temperature, net radiation) were distributed over the terrain, using a combination of geometric models [Dozier and Frew, 1990] and interpolation between point measurements [Colee *et al.*, 2000], with net radiation calculated using both SADF and AADF. Catchment-wide discharge data were available from a stream gage (Figure 1).

[7] Modeled melt fluxes were also summed to estimate the initial SWE of each pixel following the methods of Cline *et al.* [1998]. Initial SWE was measured during an extensive field campaign (6–12 April 1997) involving over 400 snow depth measurements and 11 snow density measurements, which were previously interpolated to the 30-m grid using binary regression trees [Molotch *et al.*, 2004].

3. Results

[8] On average, 83% of observed albedo values fell within one standard deviation of the mean (Figure 2a). The SADF and basin-average AADF decay rates were 10% and 15% respectively for the first day after snowfall. After that the decay rates differed substantially (Figure 2b). Average daily decay rates for snow 2–8 days old were 7% for the SADF and 0.3% for the AADF.

[9] Catchment-wide modeled snowmelt was compared with observed discharge (Figure 3). The timing of snowmelt was simulated more accurately using the AADF (Figure 3), which results directly from the more-accurate radiative flux estimates using the AADF. The coefficient of determination (R^2) between modeled snowmelt and observed runoff was 0.73 versus 0.59 for the AVIRIS-measured versus strictly empirical albedo estimates, with no model calibration. The greatest impact on snowmelt accuracy was early in the melt season (Figure 3), after which the simulated hydrographs converged around 20 May. Figure 4 shows the differences between modeled net solar radiation over snow-covered terrain using the AADF and SADF on north-facing and south-facing regions as defined by the following northness-criterion:

$$\text{northness} = \cosine(\text{aspect}) \times \text{sine}(\text{slope}). \quad (2)$$

Where *slope* and *aspect* are in degrees and degrees from north respectively. North-facing and south-facing slopes were

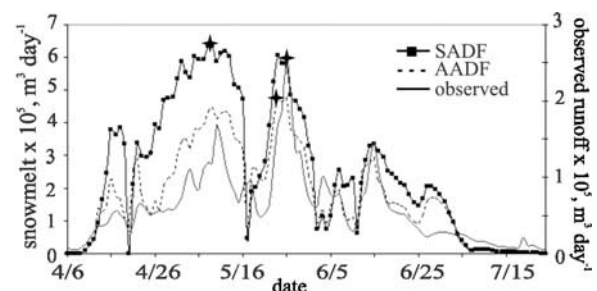


Figure 3. Observed and simulated hydrographs using both the SADF and the AADF in the snowmelt model. Stars indicate respective peak runoff.

defined as regions with $northness > 0.3$ and $northness < -0.3$ respectively. Prior to 20 May deviations in modeled net solar radiation using the SADF and AADF were greater on south-facing slopes relative to north-facing slopes (Figure 4); AADF values on south-facing slopes approach the SADF values later in the melt season.

[10] The modeled peak snowmelt occurred 18 d before the observed peak for the SADF and 2 d for the AADF model. Due to lower albedo values, the SADF model overestimates the melt flux throughout the melt season; note that SWE was not a model input and therefore total melt flux was not constrained by initial SWE.

[11] Model-estimated initial SWE was within 1 standard deviation of the mean observed SWE over 43% versus 64% of the catchment using the SADF versus the AADF (Figure 5). Over the whole melt season, the amount of modeled snowmelt differed from the observed initial SWE by 36% versus 2% using the SADF versus AADF albedo. The lower albedo values of the SADF caused snowmelt magnitude, and hence initial SWE, to be overestimated. Both simulations underestimated initial SWE in the southwestern portion of the basin, where leeward slope orientation, avalanche re-deposition, and low solar irradiance cause heavy snow accumulation.

[12] To assess the physiographic controls on the model improvement associated with using AADF versus SADF, a multivariate regression between “model improvement,” (absolute initial SWE error using SADF minus that using AADF) and two independent variables (elevation and solar irradiance) was developed. Model improvement was positively correlated with elevation and solar irradiance, with coefficients 0.06 and 0.37, respectively. An analysis of variance was significant at the 99% confidence level ($p = 0$). The independent variables were able to explain 33% of the spatial variability in model improvement. Considering elevation and solar irradiance as indices of the turbulent and radiative fluxes respectively, areas where the radiative flux dominated snowmelt showed the greatest improvement.

4. Discussion

[13] Using site-specific AVIRIS data versus a basin-wide empirical function offers 3 potential benefits for estimating albedo: i) observations provide accurate values of the spatial distribution of snow albedo, ii) decay functions can be

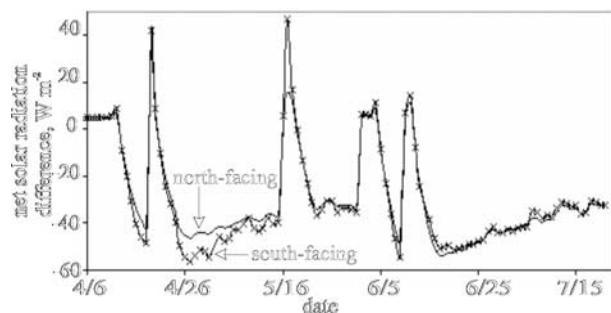


Figure 4. Daily differences between modeled net solar radiation using the AADF and SADF albedo parameterizations (AADF - SADF) on north-facing and south-facing slopes.

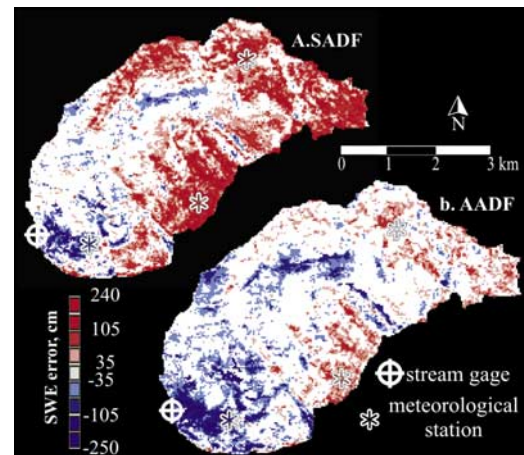


Figure 5. Error in back-calculated initial SWE estimate using the SADF (a) and AADF (b) to model snowmelt. White areas are within 1 standard deviation of the mean observed SWE. Red and blue areas represent model overestimates and underestimates respectively.

developed for each physiographically different part of the catchment to estimate albedo between acquisition dates, and iii) site-specific decay functions result in more accurate albedo estimates than universal decay functions. When albedo retrieval methods are improved for MODIS data, they will have poorer spatial resolution (500 m) but 1 d temporal resolution, thus providing much better time-series data on albedo decay. Physically based models of albedo decay, based on radiative transfer in the snowpack [Wiscombe and Warren, 1980], coupled with an energy-balance model of grain growth, currently under development [Davis *et al.*, 1993], offer a complementary approach to improving spatial albedo estimates over time.

[14] The lower albedo estimated using the SADF versus AADF, and hence greater modeled absorption of solar radiation by the snowpack could be due to the presence of vegetation-induced shading of the snow surface and anthropogenic dust sources at the sites used to derive the SADF [U.S. Army Corps of Engineers, 1956]. Although the SADF was derived at a location close to the Tokopah catchment, relative to the distance of other areas where the SADF has been used, the physiographic conditions controlling albedo decay rates (i.e., elevation, aspect, and vegetation) are extremely different in the Tokopah catchment and the sites used to derive the SADF. Therefore the SADF may not accurately represent albedo decay rates in areas outside of the narrow range of conditions at the sites used to derive the function.

[15] Small differences in albedo had the greatest impact on melt flux in areas where solar irradiance contributed most significantly. Thus the melt flux simulations did not deviate as much on north-facing slopes despite considerable variability between SADF and AADF albedo values (Figures 6a and 6b). At peak runoff, differences between snowmelt estimated using SADF versus AADF were greatest in areas exposed to greater solar irradiance (Figure 6b).

[16] The greater underestimate of snowmelt obtained using the AADF in the southwestern portions of the catchment probably results from underestimates of incoming longwave radiation. Steep cliffs are bare of snow

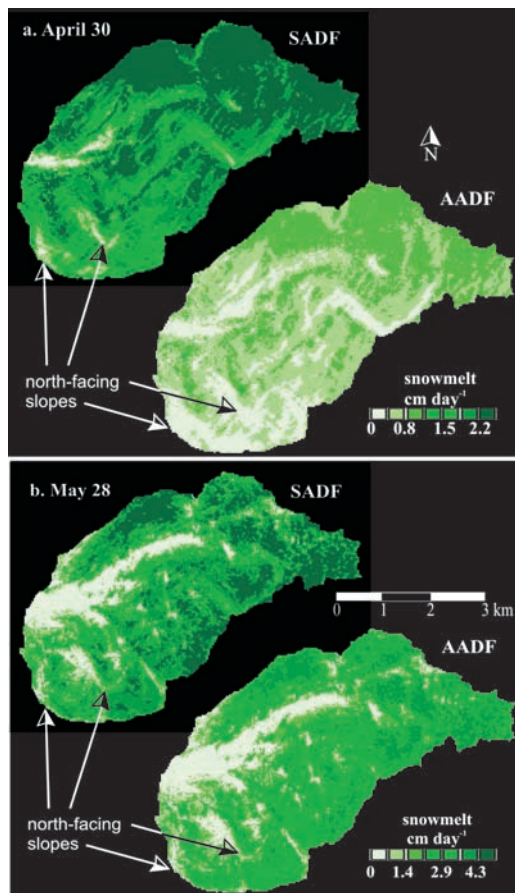


Figure 6. The spatial distribution of modeled snowmelt during low flow (30 April 1997) (a) and at peak runoff (28 May 1997) (b).

throughout the winter, becoming a major source of incoming longwave radiation to surrounding terrain. The lower albedo values of the SADF enhanced the downward flux of shortwave radiation, making up for underestimates in the downward longwave component and resulting in more accurate snowmelt estimates. This result is considered to be a coincidental artifact of the modeling procedure and not indicative of a more accurate representation of the energy exchange processes.

5. Conclusions

[17] For this alpine catchment, which is typical of the deep snowpacks and relatively high albedo found above timberline in the western U.S., albedo estimated using a common empirical method gave values that were considerably lower than values estimated from remotely-sensed measurements made over the catchment. Using the distributed albedo estimates in a snowmelt model that explicitly includes net solar radiation resulted in a significantly more accurate estimate of the timing and magnitude of snowmelt in the catchment, as compared to using

the same model with the spatially constant empirical albedo. Differences were most significant in the higher elevation areas with high incident solar irradiance, which correspond to areas where radiative fluxes dominate the snowmelt.

[18] Applications using remotely-sensed albedo should be most effective where solar radiation dominates the melt flux, such as mid-latitude alpine terrain and mid-latitude mountain plateaus. Accurate information early in the melt season, when solar radiation is more important than other energy fluxes, is more valuable for operational runoff forecasts than later in the melt season, when turbulent transfer becomes more important.

[19] **Acknowledgments.** Financial support was provided by NASA Grant NAG5-4514 and the National Science Foundation Agreement No. EAR-9876800. Michael Colee and Walter Rosenthal provided technical support. The authors are indebted to all who participated in the data collection. Comments from two anonymous reviewers are acknowledged with thanks.

References

- Blöschl, G. (1991), The influence of uncertainty in air temperature and albedo on snowmelt, *Nordic Hydrology*, 22(2), 95–108.
- Blöschl, G., D. Gutknecht, and R. Kirnbauer (1991), Distributed snowmelt simulations in an alpine catchment, 2. Parameter study and model predictions, *Water Resour. Res.*, 27(12), 3181–3188.
- Brubaker, K., A. Rango, and W. Kustas (1996), Incorporating radiation inputs into the snowmelt runoff model, *Hydrological Processes*, 10(10), 1329–1343.
- Cline, D. W., R. C. Bales, and J. Dozier (1998), Estimating the spatial distribution of snow in mountain basins using remote sensing and energy balance modeling, *Water Resour. Res.*, 34(5), 1275–1285.
- Colee, M. T., T. H. Painter, W. Rosenthal, and J. Dozier (2000), A spatially distributed physical snowmelt model in an alpine catchment, *Proceedings, Western Snow Conference*, 68, 99–102.
- Davis, R. E., A. W. Nolin, R. Jordan, and J. Dozier (1993), Towards predicting temporal changes of the spectral signature of snow in visible and near-infrared wavelengths, *Annals of Glaciology*, 17, 143–148.
- Dozier, J., and J. Frew (1990), Rapid calculation of terrain parameters for radiation modeling from digital elevation data, *IEEE Transactions on Geoscience and Remote Sensing*, 28(5), 963–969.
- Klein, A. G., and J. Stroeve (2002), Development and validation of a snow albedo algorithm for the MODIS instrument, *Annals of Glaciology*, 34, 45–52.
- Molotch, N. P., R. C. Bales, M. T. Colee, and J. Dozier (2004), Estimating the spatial distribution of snow water equivalent in an alpine basin using binary regression tree models: The impact of digital elevation data and independent variable selection, *Hydrol. Proc.*, in press.
- Painter, T. H., J. Dozier, D. A. Roberts, R. E. Davis, and R. O. Green (2003), Retrieval of subpixel snow-covered area and grain size from imaging spectrometer data, *Remote Sensing of Environment*, 85(1), 64–77, doi:10.1016/S0034-4257(02)00187-6.
- U.S. Army Corps of Eng. (1956), *Snow Hydrology: Summary Report of the Snow Investigations*, 462 pp., North Pacific Division, Corps of Eng., Portland, OR.
- Wiscombe, W. J., and S. G. Warren (1980), A model for the spectral albedo of snow, I, Pure snow, *J. Atmospheric Sciences*, 37(12), 2712–2733.

- N. P. Molotch, Department of Hydrology and Water Resources, University of Arizona, Tucson, AZ, USA. (smolotch@hwr.arizona.edu)
- T. H. Painter, National Snow and Ice Data Center, University of Colorado, Boulder, CO, USA. (tpainter@nsidc.org)
- R. C. Bales, Division of Engineering, University of California, Merced, CA, USA. (rbales@ucmerced.edu)
- J. Dozier, Donald Bren School of Environmental Science and Management, University of California, Santa Barbara, CA, USA. (dozier@bren.ucsb.edu)